RESEARCH ARTICLE | DECEMBER 09 2022

Chemical reactivity under collective vibrational strong coupling

Derek S. Wang ✉ ; Johannes Flick ; Susanne F. Yelin

J. Chem. Phys. 157, 224304 (2022)
https://doi.org/10.1063/5.0124551

The Journal of Chemical Physics ARTICLE scitation.org/journal/jcp

Chemical reactivity under collective vibrational strong coupling

Cite as: J. Chem. Phys. 157, 224304 (2022); doi: 10.1063/5.0124551
Submitted: 6 September 2022 • Accepted: 18 November 2022 •
Published Online: 9 December 2022

Derek S. Wang,[1,a] Johannes Flick,[2,3,4,b] and Susanne F. Yelin[5,c]

AFFILIATIONS

[1] Harvard John A. Paulson School of Engineering and Applied Sciences, Harvard University, Cambridge, Massachusetts 02138, USA
[2] Center for Computational Quantum Physics, Flatiron Institute, New York, New York 10010, USA
[3] Department of Physics, City College of New York, New York, New York 10031, USA
[4] Department of Physics, The Graduate Center, City University of New York, New York, New York 10016, USA
[5] Department of Physics, Harvard University, Cambridge, Massachusetts 02138, USA

[a] **Author to whom correspondence should be addressed:** derekwang@g.harvard.edu
[b] **E-mail:** jflick@flatironinstitute.org
[c] **E-mail:** syelin@g.harvard.edu

ABSTRACT

Recent experiments of chemical reactions in optical cavities have shown great promise to alter and steer chemical reactions, but still remain poorly understood theoretically. In particular, the origin of resonant effects between the cavity and certain vibrational modes in the collective limit is still subject to active research. In this paper, we study the unimolecular dissociation reactions of many molecules, collectively interacting with an infrared cavity mode, through their vibrational dipole moment. We find that the reaction rate can slow down by increasing the number of aligned molecules, if the cavity mode is resonant with a vibrational mode of the molecules. We also discover a simple scaling relation that scales with the collective Rabi splitting, to estimate the onset of reaction rate modification by collective vibrational strong coupling and numerically demonstrate these effects for up to 10^4 molecules.

Recent studies in the field of vibrational polariton chemistry suggest that chemical reactivity—such as reaction rates,[1] product selectivity,[2] and charge–transfer equilibrium[3]—can be modified by coupling the dipole moments of molecular vibrational modes to the vacuum electric field of infrared cavity modes. Despite intense efforts to develop a theory of vibrational polariton chemistry (see, e.g., Refs. 4–18), a comprehensive explanation remains elusive.

While assuming uncoupled harmonic molecular vibrational modes is computationally convenient for analytical and numerical models, chemical reactions such as dissociation inherently involve the full exploration of anharmonic and coupled vibrational potentials, which can profoundly impact reaction dynamics.[19,20] In fact, recent computational studies[10,14] using *ab initio* or classical models of chemical reactivity in a cavity show that cavity coupling can modify the reaction dynamics by interfering with the intramolecular vibrational energy redistribution (IVR), which is feasible only when the coupled and anharmonic nature of vibrational modes is taken into account.

In these studies, however, only a single molecule coupled to a cavity has been considered. To match the single-molecule Rabi splitting with the collective Rabi splitting observed in experiment, these theoretical studies require vacuum electric fields, leading to the light–matter coupling strength being much larger than that experimentally realizable in optical cavities. It is still an open question how insights from predictions for single-molecule scenarios translate to the experimentally relevant case of many molecules. On the other hand, the development of cavity molecular dynamics simulations[21] that consider up to thousands of molecules has yielded novel insights into the cavity-modified excitation and relaxation dynamics, but not yet addressed changes in chemical reactivity.

In this work, we study changes in the chemical reactivity when many molecules are collectively coupled to an infrared cavity.

For collections of aligned molecules with energies greater than the dissociation threshold, we find that the reaction rate can be slowed down when the optical cavity mode is tuned in resonance with the vibrational mode. In this case, the collective vibrational state of the many molecules drives the cavity displacement, enabling cavity-mediated vibrational energy distribution as fast as IVR processes. This effect remains even when there is only one molecule energetic enough to react in a bath of many less energetic molecules, conditions that are closer to experimental setups in thermal equilibrium. When we consider randomly oriented molecules, however, changes to the chemical reactivity largely disappear, due to the light–matter coupling that scales more weakly with the number of molecules than in the aligned case, suggesting that further investigations are necessary to better understand the origin of cavity-modified ground state chemical reactivity.

In this work, we study a simple, classical model for the vibrational dynamics of N_{mol} molecules, collectively coupled to an optical cavity, taking into account the anharmonicity of the chemical bonds. We schematically illustrate this model in Fig. 1. The total Hamiltonian can be written as $H = H_{\mathrm{mol}} + H_{\mathrm{F}}$, where the molecular Hamiltonian H_{mol} and the field Hamiltonian H_{F} are given by

$$H_{\mathrm{mol}} = \sum_{n=1}^{N_{\mathrm{mol}}} \left[\sum_{i=1}^{3} \left(\frac{1}{2} G_{ii}^{(0)} p_{n,i}^2 + V_{n,i}(q_{n,i}) \right) + \sum_{i,j}^{3} G_{ij}^{(0)} p_{n,i} p_{n,j}, \right], \quad (1a)$$

$$H_{\mathrm{F}} = \frac{1}{2} P_{\mathrm{c}}^2 + \frac{1}{2} \omega_{\mathrm{c}}^2 \left(Q_{\mathrm{c}} - \frac{\lambda_{\mathrm{c}}}{\omega_{\mathrm{c}}} \boldsymbol{\mu} \cdot \boldsymbol{\xi} \right)^2. \quad (1b)$$

In the molecular Hamiltonian H_{mol}, each molecule n is represented by a classical triatomic model with three degrees of freedom $(q_{n,i})$ and anharmonic potentials $(V_{n,i})$. Previously used as a minimal model for the emergence of anharmonicity and chaos in IVR,[22–24] this model was extended recently to describe the chemical reactivity of a single molecule in an infrared optical cavity.[14] We briefly review the molecular model: $i = \{1, 2\}$ that corresponds to the local stretching modes, and $i = 3$ is the local bending mode. For the two stretching modes, the vibrational potentials are approximated by Morse potentials $(V_{n,i} = D\{1 - \exp[-\alpha_i(q_{n,i} - q_i^0)]\}^2)$, where D is the dissociation energy and q_i^0 is the equilibrium position. For the bending mode, the vibrational potential is assumed to be harmonic: $V_{n,3} = \omega_3^2 (q_{n,3} - q_3^0)^2 / (2G_{33}^{(0)})$. The definitions and numerical values for these parameters correspond to those of an ozone-like molecule and are provided in Refs. 14 and 24. Notably, the local vibrational modes $q_{n,1}, q_{n,2}$, and $q_{n,3}$ are coupled through the vibrational momentum mode–mode coupling terms $G_{ij}^{(0)}$, resulting in three normal modes (normal bending, symmetric stretching, and anti-symmetric stretching).

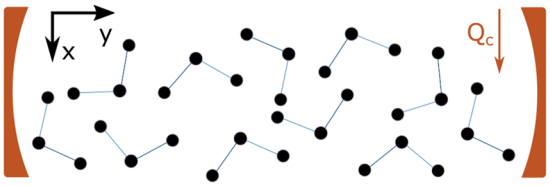

FIG. 1. Schematic of N_{mol} molecules coupled to an infrared cavity. Each molecule n comprises three local vibrational modes: anharmonic stretch $q_{n,1}$, anharmonic stretch $q_{n,2}$, and harmonic bend $q_{n,3}$. We fix the orientation θ_n between the cavity displacement Q_{c} and the molecular axis.

In the field Hamiltonian H_{F}, the variables ω_{c}, Q_{c}, P_{c}, and λ_{c} are the frequency, displacement, momentum, and strength of the cavity mode "c;" $\boldsymbol{\mu} = \sum_{n=1}^{N_{\mathrm{mol}}} \boldsymbol{\mu}_n = \mu_x \hat{x} + \mu_y \hat{y}$ is the permanent dipole moment of the N_{mol} molecules; $\boldsymbol{\xi}$ is the unit vector of polarization of the electric field; θ_n is the angle between the molecular axis and x-axis. The parameterization of the permanent dipole moment $\boldsymbol{\mu}_n$ is described in Appendix A.

Finally, to focus on the direct molecule–cavity coupling, we neglect potentially relevant molecular translations and rotations, intermolecular dipole–dipole and dispersion interactions, and photon loss through the cavity, respectively, although the presence of the cavity may impact these other terms as well.

We can then stably propagate the equations of motion derived from H with Hamilton's equations, using the eighth order Runge–Kutta method.[25] A molecule is considered dissociated when the bond length of either local stretch modes in a molecule exceeds five Bohr from equilibrium—a criterion originally applied in Ref. 24 and chosen because the dissociation probabilities converge at this bond length. Because the dissociation dynamics depend on the initial state, we average over many ensembles, generated as described in Appendix B, for the results presented here. Briefly, for results shown in the main text, each molecule in an ensemble of N_{mol} molecules is initialized in a randomly chosen state with a given energy. Other initializations are possible; for instance, we explore the effect of coherently initializing all molecules in an ensemble with the same initial state in the Appendix. With this approach, in Ref. 14 for the single-molecule case, we find that when the optical cavity is resonantly coupled to particular anharmonic vibrational modes, the cavity can interfere with IVR and alter unimolecular dissociation reaction rates, by acting as a reservoir for vibrational energy.

To investigate how the chemical reactivity changes under collective vibrational strong coupling, in Fig. 2(a), we initialize ensembles of N_{mol} excited molecules in a cavity and monitor their reaction rate. Each molecule has an initial energy of 34 kcal/mol > D, where D = 24 kcal/mol is the dissociation energy, and we plot the time-dependent survival probability S, or the ratio between the number of undissociated molecules and total molecules, for N_{mol} up to 10^4. The chosen cavity frequency $\omega_{\mathrm{c}} = 520\ \mathrm{cm}^{-1}$ results in the maximum change in chemical reactivity for this molecular model when $N_{\mathrm{mol}} = 1$ and $\theta = 0$, corresponding to the normal bending model that serves as a vibrational energy reservoir for the dissociating stretch modes,[14] and the cavity strength $\lambda_{\mathrm{c}} = 8 \cdot 10^{-4}$ atomic units (a.u.) for $N_{\mathrm{mol}} = 10^4$ results in a collective Rabi splitting magnitude of ~10% of the vibrational mode frequency, well within the range of experimental values. We find that the reaction slows down drastically for $N_{\mathrm{mol}} > 10^2$–10^3 and that this slowdown becomes more pronounced with increasing N_{mol}.

To understand how cavity the changes the reaction rate under collective vibrational strong coupling, in Fig. 2(b) for the same $\lambda_{\mathrm{c}} = 8 \cdot 10^{-4}$ a.u., $\omega_{\mathrm{c}} = 520\ \mathrm{cm}^{-1}$, and $N_{\mathrm{mol}} = 2 \cdot 10^3$, we plot the distribution of energy per molecule of the cavity-molecule system within the first 0.2 ps for the following degrees of freedom: the average energy per short-lived $(0.5 < t_{\mathrm{dis}} < 1$ ps) or long-lived

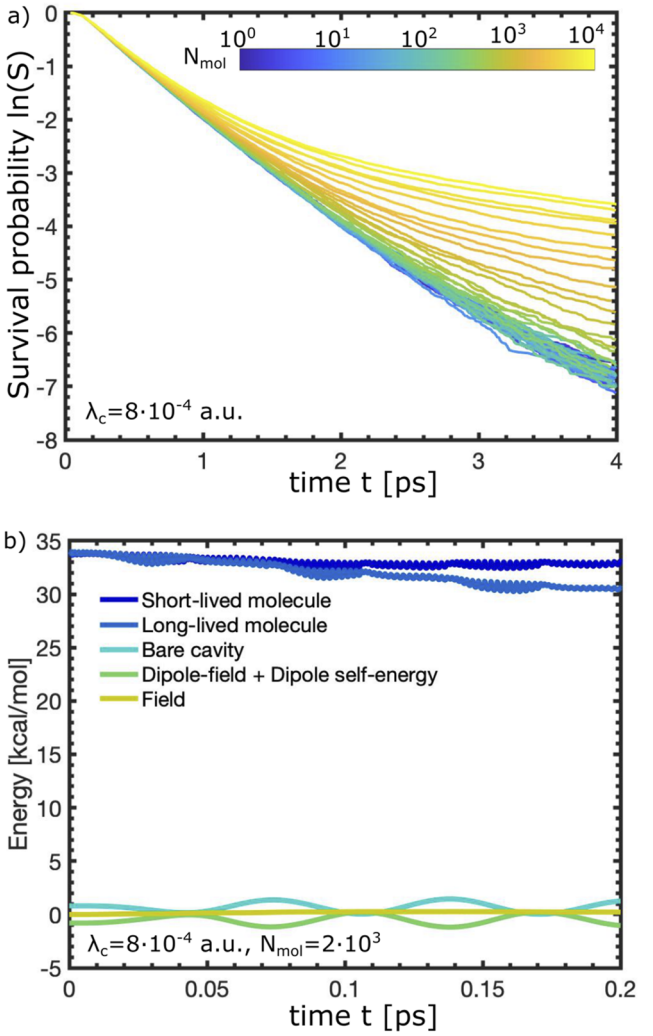

FIG. 2. (a) Reaction progress measured with time-dependent survival probability S. Increasing the number of molecules N_{mol} for constant cavity strength λ_c and cavity frequency ω_c = 520 cm^{-1} decreases the reaction rate. (b) Energy distribution for $\lambda_c = 8 \cdot 10^{-4}$ atomic units (a.u.) and $N_{mol} = 2 \cdot 10^3$. The change in the reaction rate can be attributed to cavity-mediated vibrational energy transfer, where decreases in molecular energy result in longer dissociation times or slower reaction rates and vice versa.

(t_{dis} > 4 ps) molecule, the bare cavity energy $(\frac{1}{2}P_c^2 + \frac{1}{2}\omega_c^2 Q_c^2)/N_{mol}$, the dipole-field and dipole-field energy $(-\omega_c\lambda_c\mu_x Q_c + \lambda_c^2\mu_x^2/2)/N_{mol}$, and the total field energy H_F/N_{mol}. The average energy of short-lived molecules decreases only slightly, while the average energy of long-lived molecules drops a couple of kcal/mol. Oscillations in the bare cavity energy are correlated with oscillations in the average energies of both short- and long-lived molecules, demonstrating femtosecond-scale energy exchange between the cavity and molecules. Just as in the single-molecule case,[14] the cavity serves as a reservoir of vibrational energy. This process can be mechanistically explained as follows: as the N_{mol} molecules vibrate, they displace the cavity displacement Q_c, the magnitude of which increases with N_{mol} for a given λ_c. Larger Q_c magnitudes enable transiently larger forces on the molecular coordinates that interfere with the bare intramolecular vibrational dynamics. Overall, here, we explicitly observe that vibrational strong coupling between many molecules and a cavity mode can augment the energy transfer between molecules through the collectively driven cavity displacement.

Next, we empirically discover an asymptotic scaling law for the onset of reaction rate modification by collective vibrational strong coupling shown in Fig. 3(a). Here, we show the cavity frequency ω_c-dependent survival probability after 1 ps for varying N_{mol} from 1 to 3000, while holding $\lambda_c(N_{mol})^{1/2}$ constant at 0.07 a.u. Notably, the curves converge as $N_{mol} > 10^2$, suggesting that in the limit of many molecules, $\lambda_c(N_{mol})^{1/2}$ dictates the effect of collective vibrational coupling on the chemical reactivity for the aligned

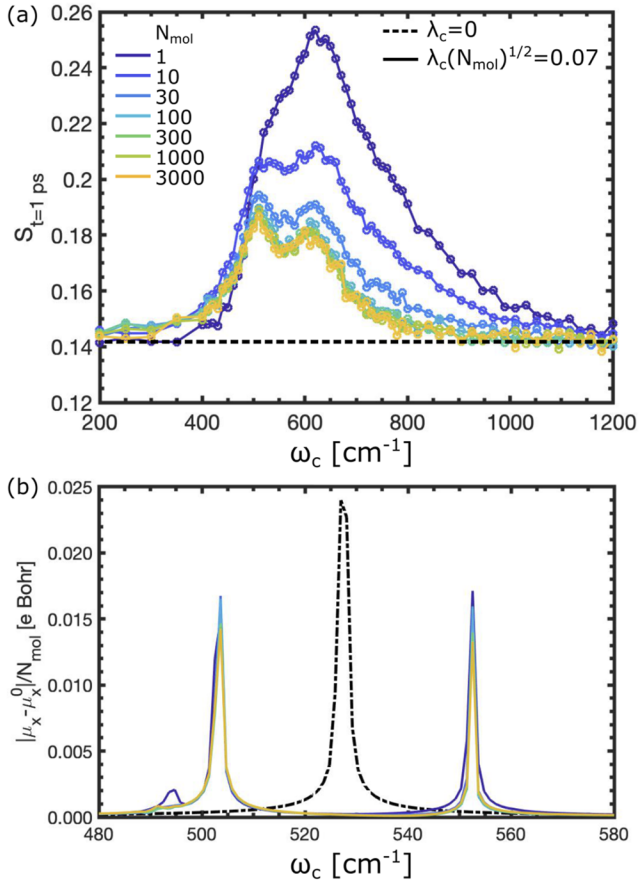

FIG. 3. (a) Resonance effect. The chemical reactivity, measured by the survival probability after 1 ps for a constant $\lambda_c(N_{mol})^{1/2}$ = 0.07 a.u., depends on the cavity frequency. The curves converge for $N_{mol} > 10^2$, suggesting that in the limit of many molecules, $\lambda_c(N_{mol})^{1/2}$ dictates the effect of collective vibrational coupling on the chemical reactivity for the aligned molecules. (b) Dipolar spectra. The collective Rabi splitting in the dipolar moment spectra scales proportionally with $\lambda_c(N_{mol})^{1/2}$. The spectra are normalized to the number of molecules N_{mol}. Here, $\lambda_c(N_{mol})^{1/2}$ = 0.07 a.u., resulting in a collective Rabi splitting of ~50 cm^{-1}, which matches the experimental values of collective Rabi splitting, albeit with fewer molecules and larger cavity strengths.

molecules. For the case of $N_{mol} = 1$, we find a broad resonance between 500 and 700 cm^{-1}. By increasing the number of molecules, we find a double peak structure at 520 and 600 cm^{-1} in the survival probability S, reminiscent of the double peaks in the vibrational infrared spectrum for long-lived trajectories of this molecular model, as shown in Ref. 14, in the limit of a single molecule. As we demonstrate in the Appendix, it appears that smaller $N_{mol} \sim 1$–10^2 have larger effective molecule–cavity couplings than those for $N_{mol} > 10^2$ for the same $\lambda_c (N_{mol})^{1/2}$, leading to the broad resonance in the survival probability. This is due to the sampling process itself, where each initial state for a molecule in an ensemble is randomly sampled separately. When the initial states are identical within an ensemble, we find that the curves overlay perfectly, even for smaller $N_{mol} \sim 1$–10^2. In Appendix F, we also demonstrate how to precisely extract this scaling law with a range of $\lambda_c (N_{mol})^{1/2}$ values.

Notably, the scaling of the survival probability with $\lambda_c (N_{mol})^{1/2}$ is identical to the scaling of the collective Rabi splitting with the number of molecules, or the change in frequency of the vibrational dynamics of the collectively coupled molecules inside vs outside a cavity, due to interactions between the molecular vibrations and the cavity. We numerically demonstrate this scaling in Fig. 3(b), where we plot the N_{mol}-normalized dipolar moment spectrum $|\mu_x - \mu_x^0|(\omega)/N_{mol} = |\int dt(\mu_x(t) - \mu_x^0)\exp(-2\pi i\omega t)|/N_{mol}$. This expression corresponds to the one-sided Fourier transform of the permanent dipole moment μ_x as the displacements q_i and momenta p_i propagate under H.

In the present system, $\lambda_c (N_{mol})^{1/2} = 0.07$ a.u. results in a collective Rabi splitting of ~50 cm^{-1}, or about 10% of the vibrational mode frequency. This regime is regularly achieved in experimental setups of vibrational polariton chemistry[1,2] and, due to cavity and molecular losses, corresponds approximately to the onset of the strong coupling regime from the weak coupling regime.

In Figs. 2 and 3, we initialize each of the molecules with an energy of 34 kcal/mol > than the dissociation energy D. In the thermal reactions of interest, however, at any given moment, only a few molecules are "hot" enough to react among a bath of colder molecules near room temperature. However, preparing thermal distributions is challenging, due to the need for large numbers of molecules and long propagation times with coupling to a thermometer. To approximate this critical feature of reactions at thermal equilibrium at room temperature, in Fig. 4, we explore whether the empirically observed scaling law remains when only one molecule is "hot" enough to react, while the rest are "cold." Specifically, we compare the survival probability after 1 ps for a single hot molecule (with total energy 34 kcal/mol > than the dissociation energy D) among $N_{mol} - 1$ cold (each with total energy of 1 kcal/mol ~43 meV, or of the order of room temperature) molecules vs ensembles where every molecule is initialized with energy 34 kcal/mol and for the "one hot" vs "all hot,"case. The former more closely corresponds to a thermal reaction at a low temperature, where there are comparatively fewer hot molecules capable of dissociating among the many cold molecules. Notably, the "one hot" case still results in N_{mol}-dependence, although the relative change in reaction rate is smaller than that for the "all hot" case. This difference is likely due to the smaller vibrational mode amplitudes of cold molecules compared to that of hot molecules, leading to relatively smaller changes

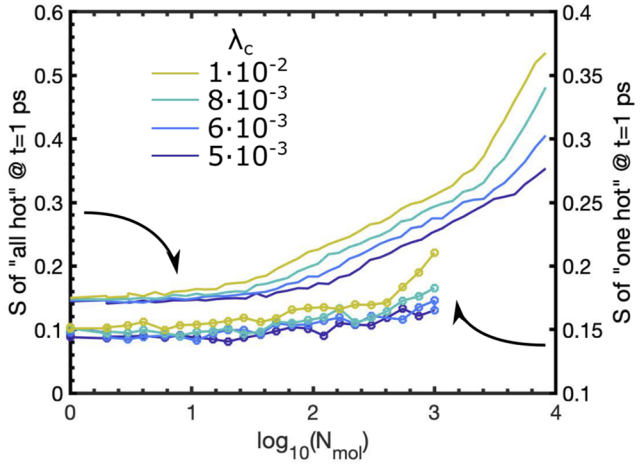

FIG. 4. Cavity-modified survival probability S after $t = 1$ ps for conditions closer to thermal reactions with varying λ_c and constant $\omega_c = 520$ cm^{-1}. We compare two cases: "one hot" (dotted with y-axis on the right), where each ensemble has one hot molecule among $N_{mol} - 1$ cold molecules, and "all hot" (lines with y-axis on the left), where each molecule in an ensemble is hot. The arrows point to the corresponding y-axes. Although the relative change in reaction rate with increasing N_{mol} is smaller for the "one hot" case than that for the "all hot" case, we observe similar changes in reaction rate with increasing N_{mol}.

in dipole moment and less coupling with the cavity. Nevertheless, this result suggests that the observed scaling law between λ_c and N_{mol} still holds for hot reacting molecules in a bath of cold molecules. To confirm that the modified chemical reactivity is a result of vibration-cavity resonance in the "one hot" case, in Appendix D., we show that the chemical reactivity is not modified by collective coupling when the cavity is off-resonant.

In Figs. 2 and 3, we also assume that the molecules are aligned along the field of the cavity mode with frequency ω_c. In most experimental studies of vibrational polariton chemistry, however, the reactants are in the liquid phase with weak orientational preferences.[21] Therefore, we randomly orient the molecules by uniformly sampling θ_n from 0 to 2π, randomly initialize each molecule with an energy of 34 kcal/mol, and study the N_{mol}-dependent survival probability S for varying λ_c shown in Fig. 5. In this setup, we observe no visible changes in the chemical reaction rate. We rationalize this qualitative difference in scaling between aligned and random orientations by comparing the N_{mol}-dependent dipolar spectrum of aligned molecules in Fig. 3(b) with that of the randomly oriented molecules in the inset of Fig. 5. First, we note that the effective λ_c in the randomly oriented case is scaled down by a factor of $\sqrt{2}$ relative to the aligned case, as can be seen in the Rabi splitting of 35 vs 50 cm^{-1} in the aligned case; this scaling can be straightforwardly derived from, for instance, the Dicke model of randomly oriented dipoles.[26] Second, and also important for observing collective enhancements of chemical reactivity, while the magnitude of the total dipolar spectrum for the aligned molecules scales proportionally with increasing N_{mol}, the magnitude of the total dipolar spectrum for the randomly oriented molecules scales only with $N_{mol}^{1/2}$. Recalling that the cavity mode Q_c couples to the total dipole moment, we find that this weaker scaling under random

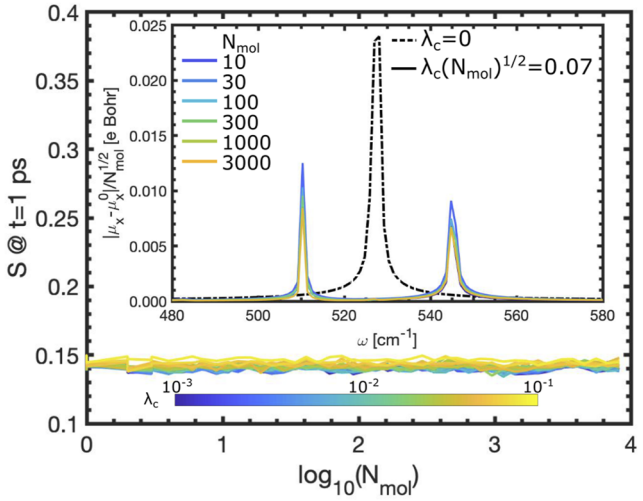

FIG. 5. Cavity-modified chemical reactivity of randomly oriented molecules, specifically N_{mol}-dependent survival S after $t = 1$ ps, with varying cavity strength λ_c and $\omega_c = 520$ cm^{-1}. Notably, there is no clear λ_c-dependent onset of N_{mol} dependence. Inset: Dipolar spectra for this limit normalized to the square-root of the number of molecules $N_{mol}^{1/2}$. Here, $\lambda_c (N_{mol})^{1/2} = 0.07$ a.u., resulting in a collective Rabi splitting of ~35 cm^{-1}.

orientation and random initialization that results in weaker per-molecule light–matter coupling, compared to the aligned setup, is evidently not capable of modifying the chemical reactivity toward large N_{mol}. Similar reduced scaling for random sampling of initial states has been found for intermolecular energy transfer in Ref. 27. We note that, we can attribute the reduced scaling to the random sampling of initial states, as shown in the Appendix in Fig. 7, where coherent initial states of randomly oriented molecules also show scaling with N_{mol}, as in the aligned case. To confirm that the modified chemical reactivity is a result of vibration cavity resonance in the "one hot" case, in Fig 8 of Appendix D, we show that the chemical reactivity is not modified by collective coupling when the cavity is off-resonant.

In summary, we study the chemical reactivity under collective vibrational strong coupling, specifically the unimolecular dissociation of a classical anharmonic triatomic model. We find that with increasing N_{mol} in the ensemble, the reaction rate decreases, due to collective enhancement of vibrational energy transfer to the cavity, as the molecules drive the cavity displacement. We empirically find a scaling relation for the onset of N_{mol}-dependence of this effect. Extrapolating this analysis to experimental conditions of smaller λ_c and larger N_{mol}, we believe that such effects may be observed in experimentally realizable infrared cavities for aligned reactants, although further study is needed to explore beyond the limit of low cavity loss and intermolecular interactions. However, because changes to the chemical reactivity are not observed for randomly oriented molecules under the significantly smaller cavity strengths of experimentally realizable cavities, we remain wary of the applicability of this theory to previous experiments of vibrational polariton chemistry with liquid phase reactants. While the findings are similar to those of Refs. 13 and 16, we note that our approach is fully classical, and that the resonance is with the vibrational transition frequency, not the barrier frequency. Future studies should explore whether the molecules can be partially aligned in realistic micron-scale cavities, whether alignment is necessary to realize collectively modified chemical reactivity, how finite cavity loss affects the observed trends, and whether collective effects can also impact the mechanism by which molecules become thermally energetic enough to react.

D.S.W. and J.F. contributed equally to this manuscript. The authors acknowledge valuable discussions with Arkajit Mandal and Tomáš Neuman. D.S.W. is an NSF Graduate Research Fellow. S.F.Y. would like to acknowledge funding by the DOE, AFOSR, and NSF for supporting the research into the molecular ensembles, for the development of numerical methods, and for the development of the theoretical formalism, respectively. Calculations were performed using the computational facilities of the Flatiron Institute. The Flatiron Institute is a division of the Simons Foundation.

AUTHOR DECLARATIONS

Conflict of Interest

The authors have no conflicts to disclose.

Author Contributions

D.S.W. and J.F. have contributed equally to this work.

Derek S. Wang: Conceptualization (equal); Data curation (lead); Formal analysis (equal); Software (lead); Visualization (equal); Writing – original draft (lead); Writing – review & editing (equal). **Johannes Flick**: Conceptualization (equal); Formal analysis (equal); Funding acquisition (equal); Investigation (equal); Resources (lead); Supervision (equal); Visualization (equal); Writing – review & editing (equal). **Susanne F. Yelin**: Formal analysis (equal); Funding acquisition (equal); Investigation (equal); Resources (equal); Supervision (equal); Writing – review & editing (equal).

DATA AVAILABILITY

The data that support the findings of this study are available from the corresponding author upon reasonable request.

APPENDIX A: DIPOLE MOMENT

We parameterize the permanent dipole moment as

$$\boldsymbol{\mu}_n = [\cos(\theta_n)\mu_{\alpha,n} + \sin(\theta_n)\mu_{\beta,n}]\hat{\boldsymbol{x}} + [\sin(\theta_n)\mu_{\alpha,n} - \cos(\theta_n)\mu_{\beta,n}]\hat{\boldsymbol{y}}, \tag{A1a}$$

$$= \mu_x\hat{\boldsymbol{x}} + \mu_y\hat{\boldsymbol{y}}, \tag{A1b}$$

where $\mu_{\alpha,n} = A\cos(q_{n,3}/2)[\mathcal{F}(q_{n,1}) + \mathcal{F}(q_{n,2})]$, $\mu_{\beta,n} = A\sin(q_{n,3}/2)[\mathcal{F}(q_{n,1}) - \mathcal{F}(q_{n,2})]$, and $\mathcal{F}(q_{n,i}) = q_{n,i}e^{-(q_{n,i}-q_i^0)^2/(2\sigma^2)}$; $\sigma = 1$ Bohr controls the envelope width, θ_n is the angle between the molecular axis and x-axis, and $A = 0.4$ e Bohr is such that the equilibrium permanent dipole moment $\boldsymbol{\mu}_0$ in the x-direction is 1 e Bohr. Importantly, the dipole moment approaches zero with increasing q_1 and q_2, physically analogous to dissociation into neutral species, to obviate challenges with the dipole approximation after dissociation.

APPENDIX B: INITIAL STATES

We briefly review the method of generating initial states, similar to previous work in Refs. 14 and 24 for a single molecule.

For a given molecule n with energy E_{mol}, we compute the minimum $Q_{n,\mathrm{min}}$ and maximum $Q_{n,\mathrm{max}}$ possible values of $Q_n \in \{q_{n,1}, q_{n,2}, p_{n,1}, p_{n,2}, p_{n,3}\}$ corresponding to the cases when E_{mol} is contained entirely within the potential or kinetic energy associated with Q_n. Then, we generate all possible initial states from uniformly spaced arrays with N values between $Q_{n,\mathrm{min}}$ and $Q_{n,\mathrm{max}}$. For each of these states with energy less than E_{mol}, we choose the $q_{n,3} - q^0_{n,3}$ that results in a total energy of E_{mol}. To obtain converged results in this study, we choose N between 15 and 23, where larger values are necessary for survival probabilities and smaller values are sufficient for Fourier spectra and time-dependent energy curves. For each ensemble, we then randomly select from these states for each N_{mol} initial state in an ensemble. We propagate $N_{\mathrm{mol}} \cdot N_{\mathrm{traj}} > 10^4$ total trajectories for each curve in Fig. 2(a) and each data point in Figs. 3–5, 9, and 10(a). The cavity is initialized, to set the contribution from the field Hamiltonian H_{F} to 0. The effects of different initial conditions for the cavity mode are studied in further detail in Ref. 14. For the case of randomly oriented molecules in Fig. 5, for each ensemble of N_{mol} molecules, we fix the randomly selected orientations θ_n and sample randomly selected initial states over multiple trajectories.

APPENDIX C: SAMPLING SCHEMES

Here, we explore the effects of different initialization procedures. First, we study the coherent initialization for aligned molecules, motivated by the observation that in Fig. 3, the effective coupling for low $N_{\mathrm{mol}} \sim 1$–10^2, despite the fact that constant $\lambda_c(N_{\mathrm{mol}})^{1/2}$ for all N_{mol} appears to be higher than that for large $N_{\mathrm{mol}} > 10^2$. We show that this difference can be attributed to the initialization conditions, where in Fig. 3, each molecule in an ensemble of N_{mol} molecules is initialized with a different random state, whereas in Fig. 6, each molecule in an ensemble is initialized with the same state. In the latter case, we see that the cavity-modified reactivity is entirely determined by $\lambda_c(N_{\mathrm{mol}})^{1/2}$.

We also explore the scaling of the total dipolar spectrum for randomly oriented molecules that are initialized, not randomly as in the main text, but coherently "kicked" as in a linear response calculation. Specifically, we displace $q_{1,n}$ and $q_{2,n}$ from the vibrational ground state by $\epsilon\cos(\theta_n)$ for all n, where ϵ is a small value. In Fig. 7, we find that the total dipolar spectrum scales with N_{mol}, as in the aligned case that exhibits collectively enhanced chemical reactivity.

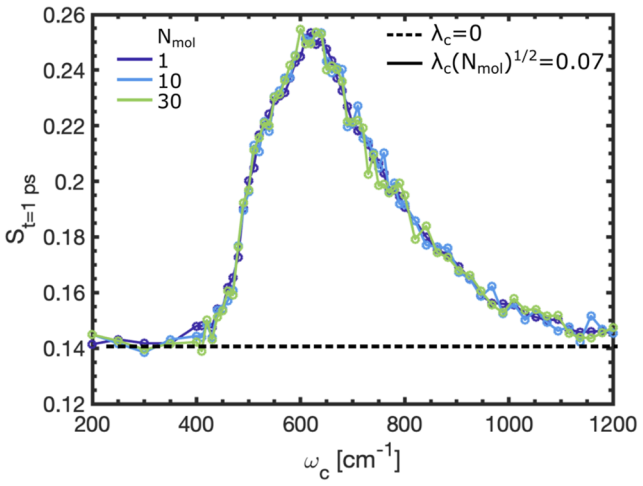

FIG. 6. Cavity frequency-dependent chemical reactivity for constant $\lambda_c(N_{\mathrm{mol}})^{1/2} = 0.07$ a.u., with aligned molecules with coherent initialization, i.e., each molecule in an ensemble has the same initial state. The curves are identical for increasing N_{mol} from $N_{\mathrm{mol}} = 1$, suggesting that under these initialization conditions, $\lambda_c(N_{\mathrm{mol}})^{1/2}$ entirely dictates the effect of collective vibrational coupling on the chemical reactivity for aligned molecules.

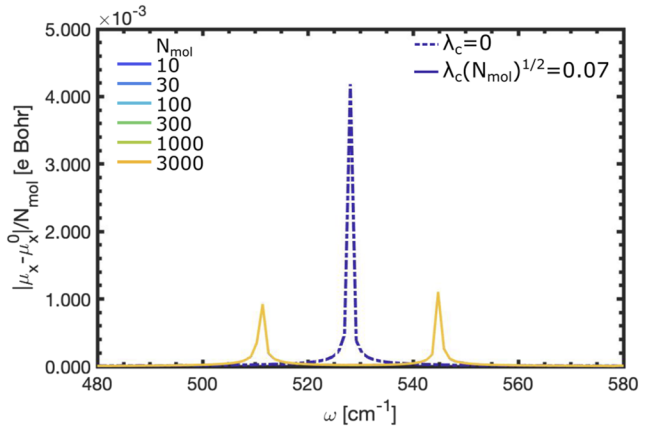

FIG. 7. N_{mol}-normalized total dipolar spectrum for randomly oriented and coherently kicked molecules in a cavity. The magnitude of the spectrum scales proportionally with N_{mol}, just as in the aligned case, in Fig. 3, that exhibits collectively enhanced chemical reactivity. All curves for $\lambda_c(N_{\mathrm{mol}})^{1/2} = 0.07$ a.u. lie on top of each other (the solid orange curve).

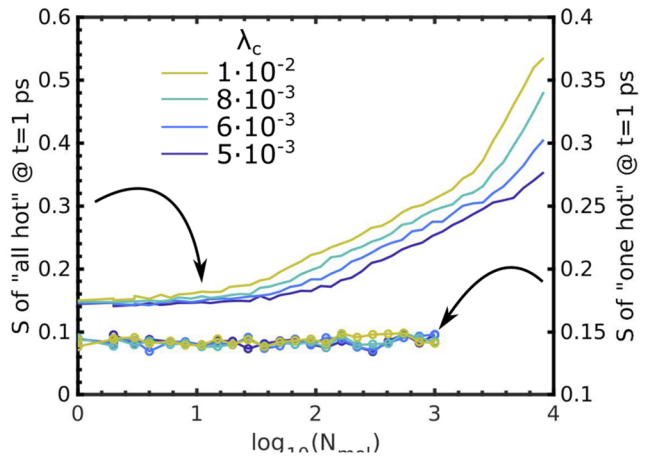

FIG. 8. The simulation parameters are identical to those in Fig. 4, except that the cavity frequency $\omega_c = 300$ cm^{-1} for the "one hot" calculation, in dotted lines, is off-resonant from vibrational resonances. The chemical reactivity is not modified when the cavity is off-resonant.

APPENDIX D: "ONE HOT" WITH OFF-RESONANT CAVITY

In Fig. 4, we find that the chemical reactivity is modified for aligned molecules, even when only one is "hot" enough to react, when the cavity frequency is resonant with particular collective vibrational resonances. Here, we show that the chemical reactivity is *not* modified when the cavity frequency is not resonant with these vibrational resonances, implying the critical role of vibration-cavity resonances.

APPENDIX E: MOLECULE NUMBER-DEPENDENT CAVITY RESONANCE

In experiments, the cavity frequency can be varied, leading to the discovery of the resonant effect where the change in reaction rate is largest at certain frequencies observed to coincide with particular vibrational modes[1–3,28] and to the original motivation for studying cavity-mediated intramolecular vibrational energy redistribution.[10,14] Therefore, in Fig. 9, we explore how the resonance frequencies change with increasing the molecule–cavity coupling. In particular, we compute the survival probability S after 1 ps with $\lambda_c = 10^{-2}$ a.u. for $N_{mol} = \{1, 30, 100, 300\}$, where the chemical reaction rate is slowed with increasing λ_c due to cavity-mediated vibrational energy transfer. As expected from Ref. 14, we observe resonances for $N_{mol} = 1$ at $\omega_c = 520$ cm^{-1} and a weaker one at $\omega_c = 600$ cm^{-1}. Interestingly, as N_{mol} increases, the resonant cavity frequencies shift, with increasing difference between the two frequencies.

APPENDIX F: SCALING RELATION FOR LARGE N_{mol}

Here, we demonstrate how we extract the scaling law $\lambda_c (N_{mol})^{1/2} = 0.07$ a.u. In Fig. 10(a), we plot the survival probability S after 1 ps of propagation, at which time the rate slowdown due to cavity-mediated intermolecular vibrational energy transfer can be clearly observed, as a function of N_{mol}, for varying λ_c. As λ_c decreases, the onset of rate slowdown occurs at increasing N_{mol}. Then, in Fig. 10(b), we plot the threshold N_{mol} at which the reaction slows down with increasing N_{mol} as a function of λ_c and overlay a fitting curve of $\lambda_c (N_{mol})^{1/2} = 7 \cdot 10^{-2}$ a.u.

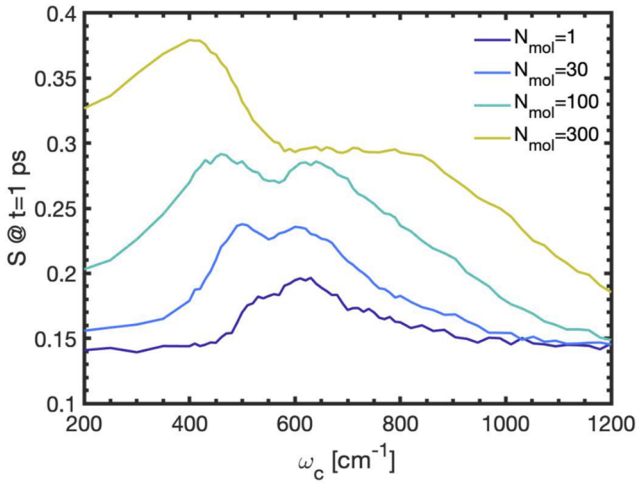

FIG. 9. Cavity frequency ω_c-dependent survival probability S after 1 ps for varying N_{mol} and $\lambda_c = 10^{-2}$ a.u. As expected, we observe a resonant effect for $N_{mol} = 1$ at $\omega_c = 520$ cm^{-1} and a weaker one at 600 cm^{-1}. As N_{mol} increases, however, the resonant cavity frequencies shift.

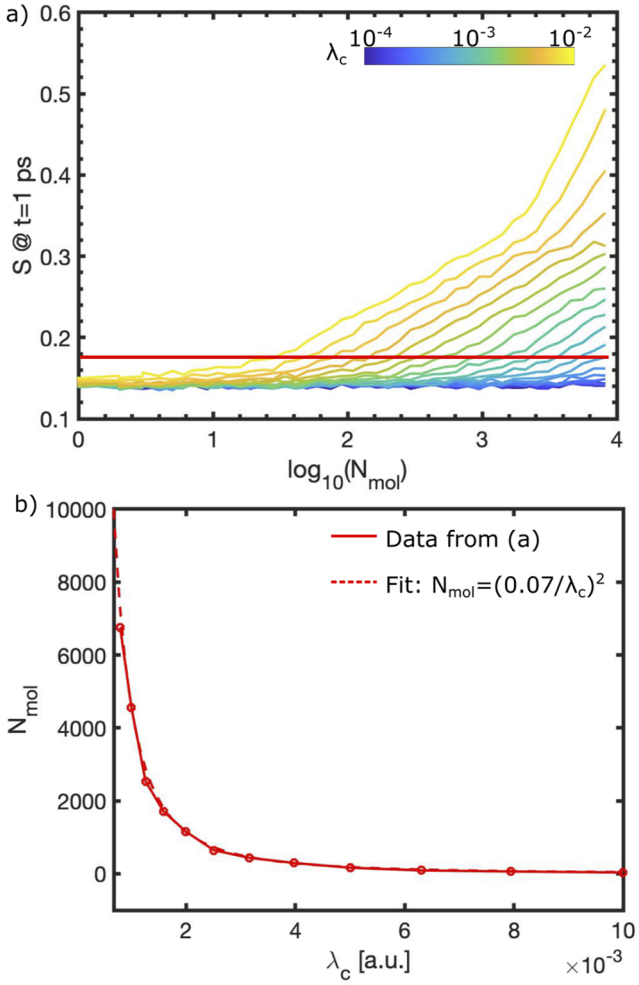

FIG. 10. (a) Survival probability after 1 ps, for constant λ_c and increasing N_{mol}. (b) Minimum N_{mol}, above which the reaction rate exhibits N_{mol}-dependence, for varying λ_c, which correspond to the points intersected by the red line in (a). We overlay a fitting curve $N_{mol} = (0.07/\lambda_c)^2$ that agrees well with the numerical data.

REFERENCES

[1] A. Thomas, J. George, A. Shalabney, M. Dryzhakov, S. J. Varma, J. Moran, T. Chervy, X. Zhong, E. Devaux, C. Genet, J. A. Hutchison, and T. W. Ebbesen, "Ground-state chemical reactivity under vibrational coupling to the vacuum electromagnetic field," Angew. Chem., Int. Ed. **55**, 11462 (2016).

[2] A. Thomas, L. Lethuillier-Karl, K. Nagarajan, R. M. A. Vergauwe, J. George, T. Chervy, A. Shalabney, E. Devaux, C. Genet, J. Moran, and T. W. Ebbesen, "Tilting

a ground-state reactivity landscape by vibrational strong coupling," Science **363**, 615 (2019).
[3]Y. Pang, A. Thomas, K. Nagarajan, R. M. A. Vergauwe, K. Joseph, B. Patrahau, K. Wang, C. Genet, and T. W. Ebbesen, "On the role of symmetry in vibrational strong coupling: The case of charge-transfer complexation," Angew. Chem. **132**, 10522 (2020).
[4]D. S. Wang and S. F. Yelin, "A roadmap toward the theory of vibrational polariton chemistry," ACS Photonics **8**, 2818–2826 (2021).
[5]J. Galego, C. Climent, F. J. Garcia-Vidal, and J. Feist, "Cavity casimir-polder forces and their effects in ground-state chemical reactivity," Phys. Rev. X **9**, 021057 (2019).
[6]J. A. Campos-Gonzalez-Angulo, R. F. Ribeiro, and J. Yuen-Zhou, "Resonant catalysis of thermally activated chemical reactions with vibrational polaritons," Nat. Commun. **10**, 4685 (2019).
[7]T. E. Li, A. Nitzan, and J. E. Subotnik, "On the origin of ground-state vacuum-field catalysis: Equilibrium consideration," J. Chem. Phys. **152**, 234107 (2020).
[8]X. Li, A. Mandal, and P. Huo, "Cavity frequency-dependent theory for vibrational polariton chemistry," Nat. Commun. **12**, 1315 (2021).
[9]X. Li, A. Mandal, and P. Huo, "Theory of mode-selective chemistry through polaritonic vibrational strong coupling," J. Phys. Chem. Lett. **12**, 6974 (2021).
[10]C. Schäfer, J. Flick, E. Ronca, P. Narang, and A. Rubio, "Shining light on the microscopic resonant mechanism responsible for cavity-mediated chemical reactivity," arXiv:2104.12429 (2021).
[11]M. Du and J. Yuen-Zhou, "Catalysis by dark states in vibropolaritonic chemistry," Phys. Rev. Lett. **128**, 096001 (2022).
[12]P.-Y. Yang and J. Cao, "Quantum effects in chemical reactions under polaritonic vibrational strong coupling," J. Phys. Chem. Lett. **12**, 9531 (2021).
[13]A. Mandal, X. Li, and P. Huo, "Theory of vibrational polariton chemistry in the collective coupling regime," J. Chem. Phys. **156**, 014101 (2022).
[14]D. S. Wang, T. Neuman, S. F. Yelin, and J. Flick, "Cavity-modified unimolecular dissociation reactions via intramolecular vibrational energy redistribution," J. Phys. Chem. Lett. **13**, 3317 (2022).
[15]W. Ahn, F. Herrera, and B. Simpkins, "Modification of urethane addition reaction via vibrational strong coupling," ChemRxiv:2022-wb6vs (2022).
[16]L. P. Lindoy, A. Mandal, and D. R. Reichman, "Resonant cavity modification of ground state chemical kinetics," J. Phys. Chem. Lett. **13**, 6580 (2022).
[17]J. Sun and O. Vendrell, "Suppression and enhancement of thermal chemical rates in a cavity," J. Phys. Chem. Lett. **13**, 4441 (2022).
[18]J. P. Philbin, Y. Wang, P. Narang, and W. Dou, "Chemical reactions in imperfect cavities: Enhancement, suppression, and resonance," J. Phys. Chem. C **126**, 14908 (2022).
[19]F. J. Hernández and F. Herrera, "Multi-level quantum Rabi model for anharmonic vibrational polaritons," J. Chem. Phys. **151**, 144116 (2019).
[20]J. F. Triana, F. J. Hernández, and F. Herrera, "The shape of the electric dipole function determines the sub-picosecond dynamics of anharmonic vibrational polaritons," J. Chem. Phys. **152**, 234111 (2020).
[21]T. E. Li, J. E. Subotnik, and A. Nitzan, "Cavity molecular dynamics simulations of liquid water under vibrational ultrastrong coupling," Proc. Natl. Acad. Sci. U. S. A. **117**, 18324 (2020).
[22]D. L. Bunker, "Monte Carlo calculation of triatomic dissociation rates. I. N_2O and O_3," J. Chem. Phys. **37**, 393 (1962).
[23]D. L. Bunker, "Monte Carlo calculations. IV. Further studies of unimolecular dissociation," J. Chem. Phys. **40**, 1946 (1964).
[24]S. Karmakar, P. K. Yadav, and S. Keshavamurthy, "Stable chaos and delayed onset of statisticality in unimolecular dissociation reactions," Commun. Chem. **3**, 4 (2020).
[25]J. R. Dormand and P. J. Prince, "High order embedded Runge-Kutta formulae," J. Comput. Appl. Math. **7**, 67 (1981).
[26]J. Keeling and P. G. Kirton, "Orientational alignment in cavity quantum electrodynamics," Phys. Rev. A **97**, 053836 (2018).
[27]T. E. Li, A. Nitzan, and J. E. Subotnik, "Collective vibrational strong coupling effects on molecular vibrational relaxation and energy transfer: Numerical insights via cavity molecular dynamics simulations," Angew. Chem. **133**, 15661 (2021).
[28]A. Sau, K. Nagarajan, B. Patrahau, L. Lethuillier-Karl, R. M. A. Vergauwe, A. Thomas, J. Moran, C. Genet, and T. W. Ebbesen, "Modifying Woodward–Hoffmann stereoselectivity under vibrational strong coupling," Angew. Chem. **133**, 5776 (2021).